

# Quantifying Scaphoid Malalignment Based Upon Height-to-Length Ratios Obtained by 3-Dimensional Computed Tomography

Paul W. L. ten Berg, MD, Johannes G. G. Dobbe, PhD, Simon D. Strackee, MD, PhD,  
Geert J. Streekstra, PhD

**Purpose** To determine if 3-dimensional height-to-length (H/L) measurements including coronal plane assessment will improve malalignment detection of scaphoid fractures and to determine if more waist than proximal pole nonunions are malaligned.

**Methods** Computed tomography scans of uninjured wrists ( $n = 74$ ) were used to obtain 3-dimensional models of healthy scaphoids. These models were used to determine 95% normal ranges of the H/L ratio in standard sagittal and coronal planes in an automated fashion. Subsequently, the H/L ratios of fibrous nonunions ( $n = 26$ ) were compared with these normal ranges and were classified as either aligned or malaligned.

**Results** The mean normal H/L ratio in the sagittal plane was 0.61 (range, 0.54–0.69) and in the coronal plane 0.42 (range, 0.36–0.48). The mean H/L ratios of the nonunions differed from those of the healthy scaphoids in these planes: 0.65 and 0.48, respectively. Based on sagittal plane evaluation of all nonunions, 46% exceeded the normal H/L range versus 54% based on combining sagittal and coronal plane measurements. More waist nonunions (71%) than proximal pole nonunions (22%) exceed the normal H/L range.

**Conclusions** Evaluation of the H/L ratio in the coronal plane provided valuable additional information for the detection of scaphoid deformities. More malaligned cases were found for waist nonunions than for proximal pole nonunions.

**Clinical relevance** This method may be a helpful diagnostic tool to detect malalignment and to choose between *in situ* fixation or reconstruction. (*J Hand Surg Am.* 2015;40(1):67–73. Copyright © 2015 by the American Society for Surgery of the Hand. All rights reserved.)

**Key words** Scaphoid deformity, scaphoid malunion, scaphoid nonunion, 3D-CT, deformity measurement.

From the Department of Plastic, Reconstructive, and Hand Surgery, the Department of Biomedical Engineering and Physics, and the Department of Radiology, Academic Medical Center, University of Amsterdam, Amsterdam, The Netherlands.

Received for publication July 29, 2014; accepted in revised form October 14, 2014.

No benefits in any form have been received or will be received related directly or indirectly to the subject of this article.

**Corresponding author:** Paul W. L. ten Berg, MD, Department of Plastic, Reconstructive, and Hand Surgery, Academic Medical Center, University of Amsterdam, Room G4-226, Meibergdreef 9, 1105 AZ Amsterdam, The Netherlands; e-mail: [paultenberg@hotmail.com](mailto:paultenberg@hotmail.com).

0363-5023/15/4001-0013\$36.00/0  
<http://dx.doi.org/10.1016/j.jhssa.2014.10.037>

A NONUNION OF THE SCAPHOID waist leads to flexion deformity and shortening, in which the proximal and distal scaphoid fragments are malaligned.<sup>1</sup>

The type of surgical treatment for correcting the deformity depends on the severity of the deformation. Slade et al<sup>2,3</sup> introduced a progressive classification for scaphoid nonunions as a guide to determine the applicability of minimally invasive procedures. When a fibrous scaphoid nonunion is only slightly malaligned, the surgeon may choose to fix the segments *in situ* by one of several *in situ* fixation techniques. For

severe deformations requiring open reduction, usually a bicortical structural bone graft is inserted before screw fixation.<sup>1</sup>

Deciding which type of correction surgery to use for a specific nonunion case requires a technique to assess the degree of scaphoid deformity. However, current 2-dimensional techniques for quantifying scaphoid deformity, such as the intrascaphoid angle (ISA), show limited reproducibility.<sup>4,5</sup> In clinical practice, an additional computed tomography (CT) scan is often obtained of the scaphoid with its long axis in the sagittal plane.<sup>6</sup> The height-to-length (H/L) ratio of the scaphoid oriented in this plane is considered the most reproducible of standard deformity measurement techniques and measures a decreased length and increased height, which are often seen in malaligned scaphoids (Fig. 1).<sup>7</sup> However, the reproducibility of height and length measurements is hampered by the scanning position of the wrist, manual selection of the most central sagittal slice, and manual measurements of height and length in CT slices. As a result, there is no consensus regarding the normal range of the H/L ratio. Some authors consider an H/L ratio greater than 0.65 as malaligned,<sup>8</sup> whereas others chose 0.60 as the cutoff value.<sup>5</sup> This may explain the absence of an unambiguous relationship between malalignment and clinical outcome.<sup>4,5</sup> Therefore, recent studies emphasize the need for reproducible techniques to measure the degree of scaphoid malalignment.<sup>4,5</sup>

A reliable evaluation technique can establish H/L ranges in healthy scaphoids and can discriminate between normally aligned (ie, not different from normal H/L ratios) and malaligned nonunions (ie, markedly different from normal H/L ratios).

Scaphoid deformability is a 3-dimensional phenomenon.<sup>9,10</sup> Standard evaluation is performed in the sagittal plane whereas a deformation may be more prominent in the coronal plane. Evaluation of the H/L ratio in both planes may therefore improve malalignment detection.

Furthermore, recent anatomical 3-dimensional CT studies report 2 different patterns of fracture displacement based on the fracture location with respect to the dorsal apex.<sup>11–14</sup> In distal fractures, the distal fragment is relatively prone to flexion, resulting in malalignment. In contrast, proximal fractures seem to be more stable.

In this study we present a CT-based method to quantify the level of malalignment using 3-dimensional modeling techniques and automated calculation of the H/L ratio in sagittal and coronal planes. We established 95% normal ranges for the H/L

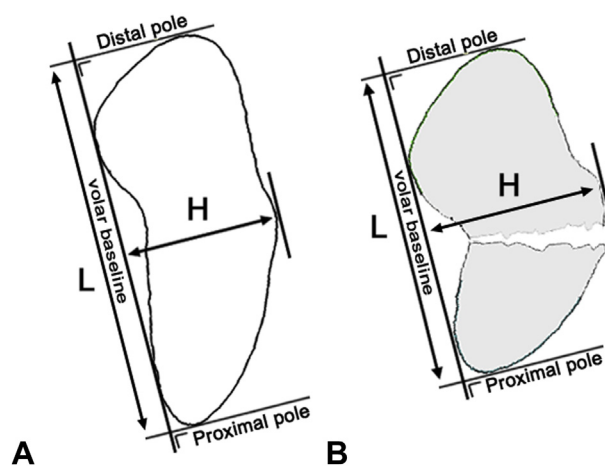


**FIGURE 1:** **A** H/L ratio of the uninjured scaphoid with anatomical shape in the sagittal plane. **B** Increased H/L ratio of a scaphoid nonunion fracture with flexion deformity and collapse, caused by decreased length and increased height.

ratio based on uninjured wrists and evaluated the discriminative power to detect malalignment in scaphoid nonunions based on our H/L calculations. We hypothesized that additional measurements in a coronal plane would improve malalignment detection in nonunions, compared with the sagittal plane alone, which is the accepted method.<sup>15</sup> We further hypothesized that proximal pole fractures are more stable and less likely to collapse, yielding normal H/L ratios.

## MATERIALS AND METHODS

### Selection of CT scans

**Healthy cases:** Images of normal scaphoids from healthy adult volunteers were obtained from bilateral CT scans used previously for anatomical studies in our department<sup>16</sup> and from the opposite healthy side of bilateral scans in cases of unilateral wrist pathologies. The healthy volunteers had no history of wrist injury or other musculoskeletal disorders. In total, 74 uninjured wrists (15 women and 32 men; average age, 31 y; range, 18–66 y) were used.

This study was approved by our human research committee. Informed consent of each individual was obtained.

**Nonunion cases:** A database search in our specialized hand surgery unit identified over 100 patients treated for various scaphoid pathologies between 2000 and 2013. Waist pseudarthroses without fibro-osseous union were excluded because of the high likelihood of independent positions of the proximal and distal fragments in relation to each other. Twenty-six fibrous nonunions were included based on operative

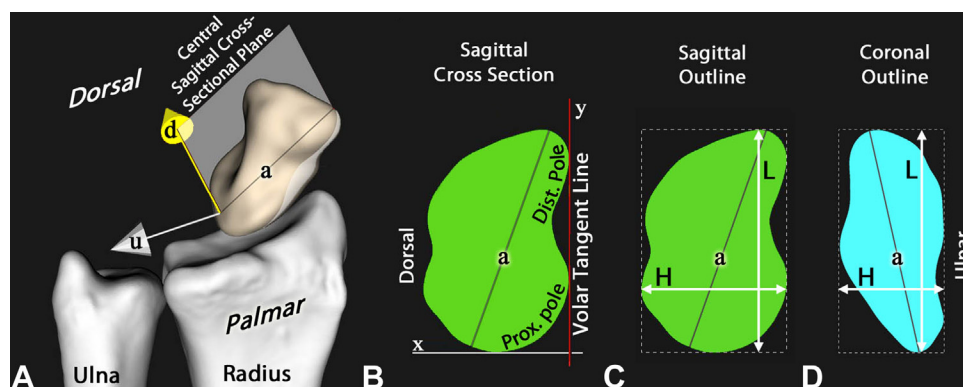


**FIGURE 2:** **A** Three-dimensional model of the scaphoid to obtain standardized sagittal and coronal cross-sections. The inertial axis pointing in the dorsal direction (*d* axis) and the longest axis (*a* axis) define the cross-sectional plane (gray panel) for making a sagittal cross-section. The inertial axis pointing in the ulnar direction (*u* axis) and the longest axis (*a* axis) define the plane (not shown) for making a coronal cross-section. **B** Scaphoid cross-section in the sagittal plane obtained using the plane in **A**. Based on the computed tangent volar baseline, a local 2-dimensional coordinate system is defined. The sagittal **C** and coronal **D** outlines (ie, bounding rectangle) provide the maximum length along the *y* axis and height along the *x* axis for calculating the H/L ratio.

reports (ie, no interfragmentary motion) and characteristics on CT scans (ie, no clear sclerotic fracture sites) acquired through dedicated standard wrist protocols.

Nonunions were separated into 17 waist injuries with stable fibrous union (3 women and 14 men; average age, 30 y; range, 16–58 y) and 9 patients with proximal pole injuries (1 woman and 8 men; average age, 25 y; range, 16–48 y). Both waist and proximal nonunions had a similar mean time of 12 months between trauma and CT scan with the exception of 1 case scanned 20 years after an injury of the proximal pole. Postoperative CT scans were analyzed, if available, to calculate postreduction H/L ratios.

#### Automated H/L computation in sagittal and coronal planes

In order to compute the H/L ratio, we automatically obtained 2-dimensional cross-sections in standardized sagittal and coronal planes from 3-dimensional virtual models of the scaphoid. This excluded variations due to scanning position of the wrist and the observer's choice of selecting a central CT slice. The cross-sections were used for automated computation of the H/L ratios, which excluded observer variability of measuring height and length (Fig. 2). The following 3 steps for computing each H/L ratio of the scaphoid were executed with our custom-made software:

**3-dimensional models and standard cross-sections:** The scaphoid was segmented from a CT scan. A 3-dimensional polygon mesh from the segmented data was derived that served as a virtual 3-dimensional model of the bone.<sup>16</sup>

Hereafter, sagittal and coronal cross-sectional planes were each defined using 2 axes in 3-dimensional space. The first axis applied to both planes and was taken as the longest axis of the scaphoid model (ie, its polygon mesh diameter), defined by the line between the 2 most distant points of the scaphoid model.<sup>17</sup> The second axis of each plane was obtained by computing the inertial axes of the scaphoid model.<sup>16,18</sup> The inertial axis pointing in the dorsal direction completed the plane for making a sagittal cross-section (Fig. 2A). The inertial axis pointing in the ulnar direction completed the plane for making a coronal cross-section.

**H/L ratio:** In order to compute height and length in the previously described cross-sections, a volar baseline (ie, tangent line) (Fig. 1) was fitted tangentially to the contours of the proximal and distal poles of the scaphoid in an automated fashion (Fig. 2B). This computed line was used as the *y* axis in a local 2-dimensional coordinate system. The horizontal *x* axis was set perpendicular to the *y* axis. The rectangle bounding the scaphoid cross-section provided height, length, and H/L (Fig. 2C).

#### Statistical analysis

Statistical analysis included determining the mean H/L ratio, its SD, the 95% normal range (mean  $\pm$  1.96 SD) and the Shapiro Wilks *W* test as a normality test. A student *t* test was used to test the difference of H/L between men and women and to test for right-to-left differences of the H/L ratio in the sagittal and coronal planes. Next, these H/L ratios in the coronal and sagittal planes were combined into a bivariate normal distribution. Using the ellipse package in *R statistics*,

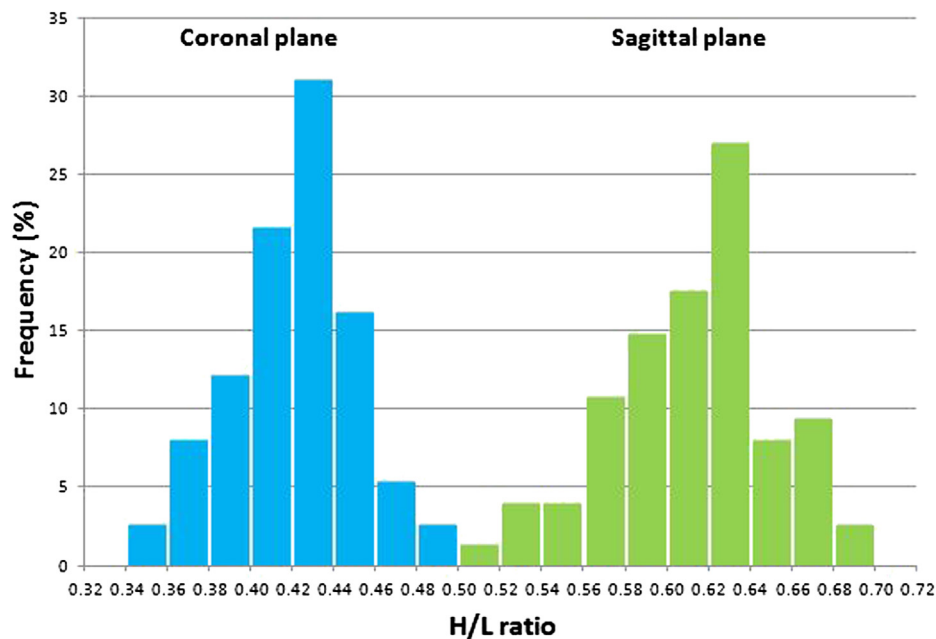


**FIGURE 3:** Distributions of the H/L ratio of uninjured scaphoids (n = 74) in the coronal plane (left) and the sagittal plane (right).

version 3.0.2 (The R Foundation For Statistical Computing, Vienna, Austria), a normal ellipse was generated, representing the 95% normal area of H/L ratios in healthy scaphoids.

Nonunions were considered malaligned (ie, non-normally aligned) if their H/L ratios exceeded the 95% normal ranges in the sagittal plane or the 95% normal ellipse, which combined the sagittal and coronal planes.

In order to evaluate the additional value of the coronal plane, we compared detection incidences of malalignment between sagittal plane (based on the 95% normal range) and both planes (based on the 95% error ellipse). To test if there was an incidence difference, a McNemar test was used.

To test if there was a difference between the detection rates of malalignment (based on the 95% error ellipse) in waist and proximal pole nonunions, a Fisher exact test was used. A 5% significance level was used for all analyses.

### Reproducibility of the method

Regarding our retrospectively analyzed CT images, different reconstruction filters were used, ranging from sharp filtering to medium filtering. In addition, although we used standard wrist protocols, complete uniformity of scanning position of the wrist among subjects could not be ensured. The type of reconstruction, the amount of random noise and the orientation of the wrist inside the scanner could have affected reproducibility of assessing the H/L ratio.

To quantify the reproducibility of assessing the H/L ratio, a single sharply filtered CT scan of an uninjured scaphoid was reoriented and resampled to simulate scanning the wrist in 4 different positions. Hereafter, these 4 simulated scans with different wrist positions were each filtered 3 times using different gaussian filters. These filters ranged from sharp to medium blurry corresponding to the patient CT scans seen in this study. Finally, the scaphoids were segmented from these 12 different CT images, and their H/L ratios were evaluated to determine the methodological variations by calculating the 95% limits of agreement ( $\pm 1.96$  SD) as interval of reproducibility.

## RESULTS

### H/L ratios in healthy scaphoids

In our sample, measurements of H/L ratios of healthy scaphoids were normally distributed in both planes (Fig. 3). The mean ( $\pm$  SD) H/L ratio in the sagittal plane was 0.61 ( $\pm 0.04$ ) with a 95% normal range from 0.54 to 0.69 and in the coronal plane 0.42 ( $\pm 0.03$ ) with a range from 0.36 to 0.48. Means of the H/L ratios between men and women were not significantly different.

### H/L ratios in nonunions

The mean ( $\pm$  SD) H/L ratio of nonunions in the sagittal plane was 0.65 ( $\pm 0.07$ ), and in the coronal plane was 0.48 ( $\pm 0.06$ ). These H/L ratios differ significantly from the normal ratios in both sagittal and coronal planes. In the sagittal plane alone, 46% of all nonunions exceeded the 95% normal range,

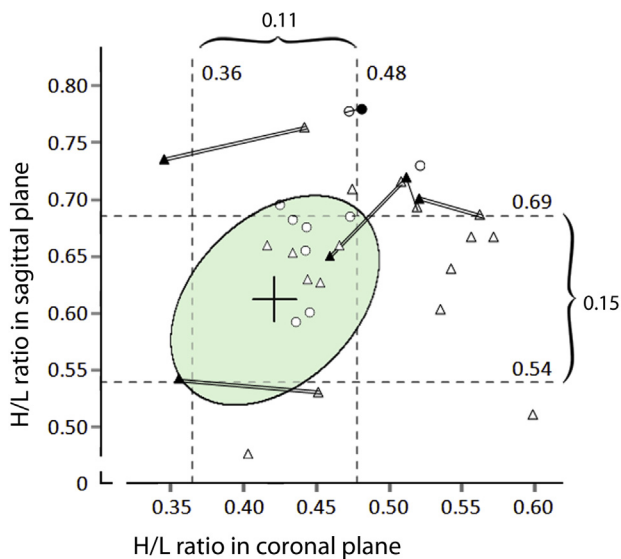


**FIGURE 4:** The mean (middle + sign) and the  $\pm 1.96$  SD limits (dashed lines) of the normal H/L ratios based on 74 uninjured scaphoids represent the normal ranges in the coronal (horizontal axis) and sagittal (vertical axis) planes separately. The ellipse represents the 95% normal range of the coronal and sagittal plane measurements combined. The open and closed triangles represent the preoperative and postoperative fibrous waist nonunions, respectively. The open and closed circles represent the preoperative and postoperative proximal pole nonunions, respectively. Pre- and postoperative values are linked by a double line when treated with cortical bone graft and by a single line when treated with cancellous bone graft. Nonunion cases within the normal ellipse are considered normally aligned.

owing to a flexion of the distal pole. Malalignment of the nonunions in the radioulnar direction was seen as well. Some cases showed normal alignment in the sagittal plane but exceeded the normal range in the coronal plane (Fig. 4), or vice versa (Figs. 4 and 5). Based on 95% normal ellipse, there was no significantly increase in the detection rate of malalignment (54%). Twelve waist nonunions (71%) exceeded the 95% normal ellipse, which was significantly more than the 2 proximal pole nonunions (22%) (Fig. 4).

Of the nonunions exceeding the error ellipse, 6 cases had postoperative CT scans enabling calculating postreduction H/L ratio. The difference in preoperative and postoperative H/L ratios was larger for the 4 nonunions treated by structural cortical bone graft and fixation (ranging from 0.01 to 0.10) than the 2 nonunion treated by cancellous bone graft and fixation (ranging from 0.0 to 0.03). In 1 case with cortical bone graft, the H/L ratios improved to normal values.

#### Reproducibility of the method

The effect of different scanning positions and different reconstruction filters yielded H/L ratios with 95% limits

of agreement in the sagittal plane of  $\pm 0.003$  and in the coronal plane of  $\pm 0.009$ . These error ranges were much smaller than natural H/L variations in healthy and pathological wrists and, therefore, ensured determining the H/L ratio with sufficient precision.

#### DISCUSSION

We presented a reproducible 3-dimensional analysis method to quantify the level of scaphoid deformity by calculating H/L ratios in standardized planes. The H/L ratios of patient cases were compared with the normal H/L ratios in healthy scaphoids. In the sagittal plane, almost 50% of our nonunion cases were considered malaligned. Malalignment was measurable not only in sagittal planes but in coronal planes as well. In some of our clinical cases, malalignment was only evident in the coronal plane. Therefore, combined assessment in both planes resulted in an increase of the malalignment detection rate, although this difference was not statistically significant. Compared with waist nonunions, significantly fewer nonunions of the proximal pole showed anomalous H/L ratios, indicating better anatomical alignment.

In 1998 Bain et al<sup>15</sup> introduced the H/L ratio as a measure for scaphoid deformity as an alternative for the ISA, which has poor reproducibility, and advocated the use of a well-defined CT scan protocol in which the wrist is held in radial deviation and neutral flexion. However, the reliability and the clinical use of the H/L ratio have been questioned for its high intra- and interobserver variability owing to variation in scanning techniques, scanning position of the wrist, and the observer's choice of the central sagittal slice.<sup>4</sup> A recent clinical interobserver study investigated the variations of H/L ratio measurements due to central slice selection using 42 CT wrist scans.<sup>5</sup> When observers chose the central slice individually, a discrepancy between central slices was observed that caused large interobserver variations resulting in a 95% limit of agreement of  $\pm 0.28$ . As a result, the clinical impact of the level of malalignment is still unclear when using this method.

In contrast to the limits of agreement in studies mentioned previously, our method proved to be highly reproducible in assessing the H/L ratio in standard planes in 3 dimensions. The 95% normal H/L range in the sagittal plane was  $\pm 0.07$ , which was 4 times smaller than the aforementioned range of interobserver variability. Our proposed normal ranges turned out to be useful in both sagittal and coronal plane to distinguish normally aligned from malaligned scaphoid nonunions, irrespective of sex.

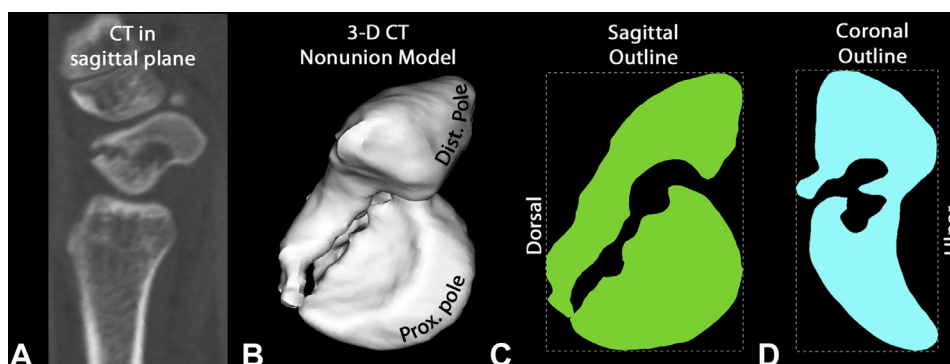


**FIGURE 5:** A, B Example of a preoperative CT scan and concomitant 3-dimensional CT model of a scaphoid waist nonunion with evident malalignment. C The outline based on a 3-dimensional model in the standard sagittal cross-section shows an H/L ratio of 18 mm/25 mm = 0.72, exceeding the normal range. D The outline in the standard coronal cross-section, showing a H/L ratio of 13 mm/26 mm = 0.51, exceeding the normal range as well.

In a comprehensive review, Barton<sup>19</sup> acknowledged that malalignment could be caused by a rotational deformity about the long axis of a scaphoid causing a deformation in the coronal plane too. Therefore, a true 3-dimensional approach provided a more complete interpretation of deformity. Recent 3-dimensional CT studies confirmed that the proximal and distal fragments can be displaced and rotated in all directions in space.<sup>11–14,20</sup> However, it requires a scanned contralateral uninjured wrist as reference, whereas our method relies on a single unilateral CT scan that requires a lower radiation dose.

These latter studies noted 2 different patterns of fracture displacement based on the fracture location with respect to the dorsal apex where the dorsal scapholunate ligaments attach.<sup>11–14</sup> In distal fractures, the bony link between the proximal and the distal rows is broken, and the distal fragment rotates into flexion. In contrast, proximal fractures seem to be more stable with less bone loss around fractures sites. Our findings support this hypothesis that fractures located proximally are more stable, showing a near-normal H/L ratio.

A limitation, however, is the relatively small number of nonunion cases in our study. In addition, there may be a geometrical limitation to detecting malaligned proximal pole fractures because, if the fragment is small enough, its rotation will not change the H/L ratio much. We were not able to calculate sensitivity, specificity, or negative and positive predictive values owing to our study design and the absence of an established reference standard for malalignment. Future studies should focus on investigating the relation between the H/L ratio with other reliable deformity parameters as relative standards and with standardized clinical outcome measurements. Another limitation was the time- and resource-intensive nature

of our method, which makes implementation in less specialized clinics or emergency departments difficult. Future software development efforts may lower the threshold for using the method.

We find that our method for H/L assessment is a valuable tool in decision making and/or evaluation in scaphoid nonunion treatment. For example, if deformity is less evident in a fibrous nonunion because of normal H/L ratios and open debridement of the fracture sites is not indicated, the surgeon could decide to fix the nonunion with *in situ* fixation without the use of an interposition bone graft.<sup>2,3</sup> To compare different treatments, a reproducible post-operative evaluation of alignment is needed as well. Cohen et al<sup>21</sup> stated that 12 waist nonunions with collapse and bone loss had restoration and maintenance of alignment with good clinical outcome using internal screw fixation with a cancellous instead of a cortical bone graft. However, alignment was assessed using the ISA, which has poor reproducibility.<sup>4,5</sup> In our study, only 2 malaligned nonunions received a cancellous bone graft. However, alignment hardly changed, and clinical outcome was poor because healing failed. In 4 nonunions receiving cortical bone graft, 1 case showed near-normal H/L ratios after surgery. Our data, although numbers are small, suggest that there is still room for improving the grafting technique and fracture reduction in future studies.

## REFERENCES

1. Buijze GA, Ochtman L, Ring D. Management of scaphoid nonunion. *J Hand Surg Am.* 2012;37(5):1095–1100; quiz 1101.
2. Slade JF III, Geissler WB, Gutow AP, Merrell GA. Percutaneous internal fixation of selected scaphoid nonunions with an arthroscopically assisted dorsal approach. *J Bone Joint Surg Am.* 2003;85(Suppl 4):20–32.

3. Slade JF III, Dodds SD. Minimally invasive management of scaphoid nonunions. *Clin Orthop Relat Res.* 2006;445:108–119.
4. Ring D, Patterson JD, Levitz S, Wang C, Jupiter JB. Both scanning plane and observer affect measurements of scaphoid deformity. *J Hand Surg Am.* 2005;30(4):696–701.
5. Forward DP, Singh HP, Dawson S, Davis TR. The clinical outcome of scaphoid fracture malunion at 1 year. *J Hand Surg Eur Vol.* 2009;34(1):40–46.
6. Sanders WE. Evaluation of the humpback scaphoid by computed tomography in the longitudinal axial plane of the scaphoid. *J Hand Surg Am.* 1988;13(2):182–187.
7. Dias JJ, Singh HP. Displaced fracture of the waist of the scaphoid. *J Bone Joint Surg Br.* 2011;93(11):1433–1439.
8. Forthman R, Jupiter JB. Scaphoid nonunion: correction of deformity with bone graft and internal fixation. *Atlas Hand Clin.* 2003;8:107–116.
9. Bhat M, McCarthy M, Davis TR, Oni JA, Dawson S. MRI and plain radiography in the assessment of displaced fractures of the waist of the carpal scaphoid. *J Bone Joint Surg Br.* 2004;86(5):705–713.
10. Smith DK. Anatomic features of the carpal scaphoid: validation of biometric measurements and symmetry with three-dimensional MR imaging. *Radiology.* 1993;187(1):187–191.
11. Moritomo H, Murase T, Oka K, Tanaka H, Yoshikawa H, Sugamoto K. Relationship between the fracture location and the kinematic pattern in scaphoid nonunion. *J Hand Surg Am.* 2008;33(9):1459–1468.
12. Moritomo H, Viegas SF, Elder KW, et al. Scaphoid nonunions: a 3-dimensional analysis of patterns of deformity. *J Hand Surg Am.* 2000;25(3):520–528.
13. Oka K, Moritomo H, Murase T, Goto A, Sugamoto K, Yoshikawa H. Patterns of carpal deformity in scaphoid nonunion: a 3-dimensional and quantitative analysis. *J Hand Surg Am.* 2005;30(6):1136–1144.
14. Nakamura R, Imaeda T, Horii E, Miura T, Hayakawa N. Analysis of scaphoid fracture displacement by three-dimensional computed tomography. *J Hand Surg Am.* 1991;16(3):485–492.
15. Bain GI, Bennett JD, MacDermid JC, Slethaug GP, Richards RS, Roth JH. Measurement of the scaphoid humpback deformity using longitudinal computed tomography: intra- and interobserver variability using various measurement techniques. *J Hand Surg Am.* 1998;23(1):76–81.
16. Vroemen JC, Dobbe JG, Jonges R, Strackee SD, Streekstra GJ. Three-dimensional assessment of bilateral symmetry of the radius and ulna for planning corrective surgeries. *J Hand Surg Am.* 2012;37(5):982–988.
17. Guo Y, Tian GL. The length and position of the long axis of the scaphoid measured by analysis of three-dimensional reconstructions of computed tomography images. *J Hand Surg Eur Vol.* 2011;36(2):98–101.
18. Leventhal EL, Wolfe SW, Walsh EF, Crisco JJ. A computational approach to the “optimal” screw axis location and orientation in the scaphoid bone. *J Hand Surg Am.* 2009;34(4):677–684.
19. Barton NJ. Twenty questions about scaphoid fractures. *J Hand Surg Br.* 1992;17(3):289–310.
20. Schweizer A, Furnstahl P, Nagy L. Three-dimensional computed tomographic analysis of 11 scaphoid waist nonunions. *J Hand Surg Am.* 2012;37(6):1151–1158.
21. Cohen MS, Jupiter JB, Fallahi K, Shukla SK. Scaphoid waist nonunion with humpback deformity treated without structural bone graft. *J Hand Surg Am.* 2013;38(4):701–705.